International Journal of Bifurcation and Chaos, Vol. 27, No. 2 (2017) 1750027 (14 pages)

DOI: 10.1142/S0218127417500274

Generating Four-Wing Hyperchaotic Attractor and Two-Wing, Three-Wing, and Four-Wing Chaotic Attractors in 4D Memristive System

Ling Zhou*, Chunhua Wang† and Lili Zhou‡
College of Computer Science and Electronic Engineering, Hunan University, Changsha 410082, P. R. China
**Department of Electronic and Information Engineering, Hunan University of Science and Engineering, Yongzhou 425199, P. R. China*
**zhouling0340@163.com*
†*wch1227164@hnu.edu.cn*
‡*joe_lily@126.com*

Received July 4, 2016; Revised October 27, 2016

By adding only one smooth flux-controlled memristor into a three-dimensional (3D) pseudo four-wing chaotic system, a new real four-wing hyperchaotic system is constructed in this paper. It is interesting to see that this new memristive chaotic system can generate a four-wing hyperchaotic attractor with a line of equilibria. Moreover, it can generate two-, three- and four-wing chaotic attractors with the variation of a single parameter which denotes the strength of the memristor. At the same time, various coexisting multiple attractors (e.g. three-wing attractors, four-wing attractors and attractors with state transition under the same system parameters) are observed in this system, which means that extreme multistability arises. The complex dynamical behaviors of the proposed system are analyzed by Lyapunov exponents (LEs), phase portraits, Poincaré maps, and time series. An electronic circuit is finally designed to implement the hyperchaotic memristive system.

Keywords: Hyperchaos; four-wing; variable-wing; memristor; circuit implementation.

1. Introduction

Chaos can be widely applied in many realms such as engineering, economy, secure communications, etc. The generation and analysis of multiwing chaotic attractors have been an important research topic. The researchers divide multiwing systems into two categories. The first category [Yu *et al.*, 2010, 2011a; Zhang & Yu, 2013] is the system with non-smooth nonlinear parts, which can generate different number of wings by increasing the number of equilibrium points with index 2. The second category [Qi *et al.*, 2008; Wang, 2009; Dadras & Momeni, 2009; Yu *et al.*, 2011a] is the system with smooth nonlinearities, in which the number of wings is not equal to that of the equilibria. Generating multiwing chaotic attractor in a smooth system has more challenge. In such an attempt, a 3D quadratic system with five equilibria was proposed in [Liu & Chen, 2003]. At first, it was believed that this system could produce a four-wing chaotic attractor. However, the same authors claimed that it was pseudo four-wing chaotic attractor but consisted

†Author for correspondence

of two coexisting and closely located double-wing attractors [Liu & Chen, 2004]. Later, the real four-wing attractors in smooth autonomous system were proposed [Qi *et al.*, 2008; Wang, 2009; Dadras & Momeni, 2009; Yu *et al.*, 2011b]. However, these systems have only one positive Lyapunov Exponent and belong to normal chaotic system.

In recent years, much effort has been made in the generation of hyperchaotic system with more complex dynamics, and hyperchaotic system can be widely applied in Secure Communication [Lin *et al.*, 2015], and encryption [Wang *et al.*, 2016]. There are few reports of hyperchaotic attractors in smooth multiwing system. The four-wing hyperchaotic attractors have been proposed by using state-feedback control and parameter trial-and-error methods [Dadras *et al.*, 2012; Zarei, 2016].

The new method to generate hyperchaotic attractor is proposed with the introduction of memristor. The memristor known as the fourth fundamental electronic element was predicted by Chua in 1971 [Chua, 1971] and firstly fabricated by Williams *et al.* [Strukov *et al.*, 2008] at HP Lab in 2008. Due to its nonvolatility, nano size, and low power consumption, the memristor has many potential applications such as neural network [Duan *et al.*, 2015; Adhikari *et al.*, 2015], nonvolatile random access memory (NRAM) [Samuel, 2016]. Recently, the dynamic behaviors of memristive nonlinear system have also been researched [Rakkiyappan *et al.*, 2015; Bao *et al.*, 2015; Wu & Wang, 2016; Bao *et al.*, 2014; Li *et al.*, 2015; Muthuswamy, 2010; Iu *et al.*, 2011; Bao *et al.*, 2011]. The analysis and design of memristive system with complex dynamics represent a big challenge. In order to realize hyperchaotic and multiwing system, Zhou proposed a memristive hyperchaotic system by replacing the resistor in modified Lü multiwing system that belongs to the first category [Zhou *et al.*, 2016]. Then, Ma proposed a memristive hyperchaotic system by adding a common smooth flux-controlled memristor and a cross-product item into a 3D pseudo four-wing chaotic system which belongs to the second category in [Ma *et al.*, 2015], and the system can only exhibit four-wing attractor, and needs an extra cross-product item. In this paper, only by adding a common smooth flux-controlled memristor, a novel memristive system can generate four-wing hyperchaotic attractor with a line of equilibria. Compared with [Ma *et al.*, 2015], due to the absence of cross-product item, it is easier to implement the circuit.

At the same time, the memristive variable-wing attractors have been presented in [Teng *et al.*, 2014; Cang *et al.*, 2016]. A memristive system using a memristor with a second-order inner state characteristic function and a fourth-degree polynomial memristance function is constructed [Teng *et al.*, 2014], and this memristor-based simplest chaotic circuit can generate a two-wing attractor and a four-wing attractor. Later, one-to-four-wing chaotic attractors are proposed in a class of simplest three-dimensional memristive systems [Cang *et al.*, 2016]. By using generalized memristor, the memristive chaotic system can generate single-scroll attractors, double-scroll attractors, and four-scroll attractors, and various coexisting attractors and hidden coexisting attractors are observed in [Yuan *et al.*, 2016]. It is very interesting to generate variable-wing attractor in memristive systems. However, the variable-attractors [Teng *et al.*, 2014; Cang *et al.*, 2016; Yuan *et al.*, 2016] are generated by the complex memristor function. In this paper, by using the easy common memristor model, the new memristive system can exhibit two-wing, three-wing, and four-wing chaotic attractors with the variation of a single parameter which denotes the strength of memristor. Moreover various coexisting multiple attractors are also observed in this system, which means extreme multistability arises. The paper is organized as follows. In Sec. 2, a novel 4D memristive system is stated. Complex dynamic behaviors of the memristive hyperchaotic four-wing system are analyzed in Sec. 3. In Sec. 4, variable-wing attractors and multiple attractors are discussed and analyzed. In Sec. 5, the circuit implementation of new memristive hyperchaotic four-wing system is proposed. Some conclusions are finally drawn in Sec. 6.

2. The 4D Memristive Four-Wing System

In 2002, Lü proposed a new double-wing system [Lü & Chen, 2002]. Later, a four-wing attractor proposed by Liu and Chen [2003] is a special case of the general Lorenz system. It can be described as follows:

$$\begin{cases} \dot{x} = \alpha x - \beta yz \\ \dot{y} = -\gamma y + xz \\ \dot{z} = xy - \delta z \end{cases} \tag{1}$$

where α, β, γ, and δ are all constants, and x, y, z are the state variables. At first, it was believed that this

system could produce a four-wing chaotic attractor, but later it was proved that the four-wing attractor was a pseudo-case as a result of the existence of the numerical artifact [Liu & Chen, 2004].

By introducing a flux-controlled memristor in the third equation of system (1), a new 4D autonomous chaotic system is given by

$$\begin{cases} \dot{x} = \alpha x - \beta yz \\ \dot{y} = -\gamma y + xz \\ \dot{z} = xy - \delta z - dW(\varphi)x \\ \dot{\varphi} = kx \end{cases} \tag{2}$$

where d is a positive parameter indicating the strength of the memristor, and $w(\varphi)$ is a memductance function. The definition of a memristor is based on the relationship between charge q and flux φ. The relationship between the voltage across a flux-controlled memristor and the current is given by the differential form shown in (3).

$$i_m = W(\varphi)v, \quad \dot{\varphi} = v. \tag{3}$$

The smooth flux-controlled memristor, which has been utilized to construct complex chaotic systems [Bao *et al.*, 2014; Li *et al.*, 2015; Muthuswamy, 2010; Iu *et al.*, 2011; Bao *et al.*, 2011], is easier to analyze and implement. The memductance function $w(\varphi)$ is shown as

$$W(\varphi) = \frac{dq(\varphi)}{d\varphi} = \frac{d(a\varphi + b\varphi^3)}{d\varphi} = a + 3b\varphi^2 \tag{4}$$

where a and b are two positive constants.

2.1. *Symmetry and invariance*

Generally, the symmetry property widely exists in dynamic system with an even number of attractors. The memristive system (2) keeps the symmetry of the original 3D system (1), and it is invariant under the transformation $(x, y, z, \varphi) \leftrightarrow (-x, y, -z, -\varphi)$. Also, attractors in state space have to be symmetric with respect to y axis.

2.2. *Equilibria and stability*

It can be seen that the equilibrium states of system (2) only rely on x, y, and z and are independent from φ. We can easily observe that the system (2) has a line equilibria $O = \{(x, y, z, \varphi) \,|\, x = y = z = 0, \varphi = c\}$, where c is any real constant.

By linearizing system (2) at point O, we can obtain the Jacobian matrix on O.

$$Jo = \begin{pmatrix} \alpha & 0 & 0 & 0 \\ 0 & -\gamma & 0 & 0 \\ -dW(c) & 0 & -\delta & 0 \\ k & 0 & 0 & 0 \end{pmatrix}. \tag{5}$$

According to the Jacobian matrix (5), the characteristic equation is given by

$$\lambda(\lambda - \alpha)(\lambda + \delta)(\lambda + \gamma) = 0. \tag{6}$$

It is very easy to solve its eigenvalues, and they can be expressed by

$$\lambda_1 = 0, \quad \lambda_2 = \alpha, \quad \lambda_3 = -\delta, \quad \lambda_4 = -\gamma. \tag{7}$$

The value of α, δ, and γ are all positive, so λ_3 and λ_4 are always negative, and λ_2 is always positive. Therefore, the system (2) has an unstable saddle point.

2.3. *Dissipativity*

The dissipativity of system (2) is described as

$$\begin{aligned} \nabla V &= \frac{\partial \dot{x}}{\partial x} + \frac{\partial \dot{y}}{\partial y} + \frac{\partial \dot{z}}{\partial z} + \frac{\partial \dot{\varphi}}{\partial \varphi} \\ &= \alpha - \gamma - \delta \end{aligned} \tag{8}$$

when α, δ, and γ satisfy $\alpha - \gamma - \delta < 0$, the system is dissipative.

3. Complex Dynamics of the Memristive Hyperchaotic Four-Wing System

In this section, the system (2) is further investigated by means of Lyapunov exponent analysis, Poincaré

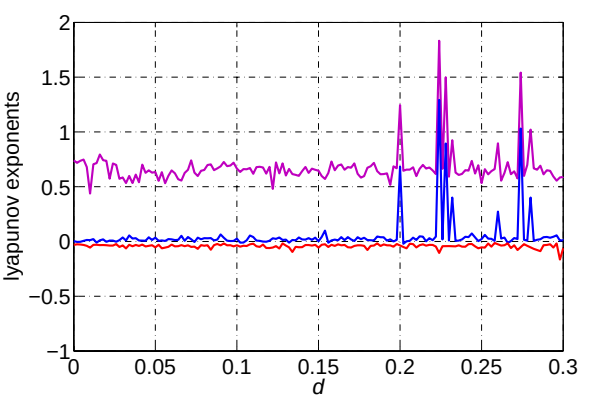

Fig. 1. LEs spectrum of system (2) versus d.

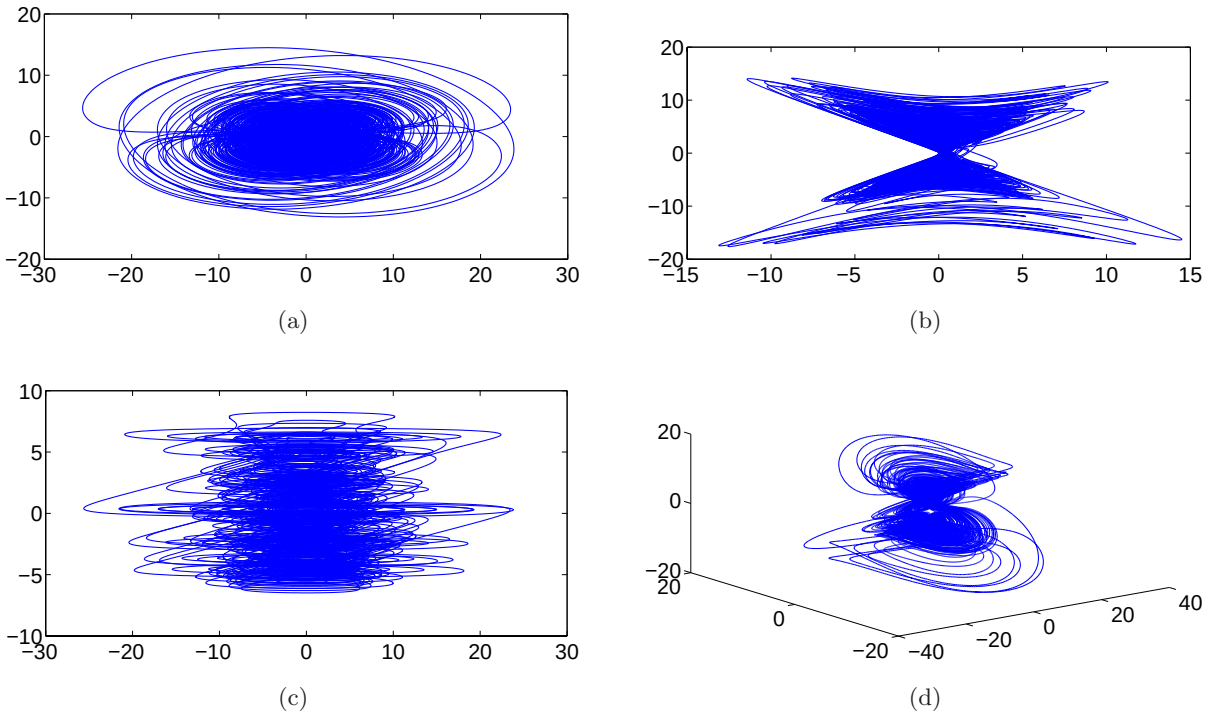

Fig. 2. Phase portraits of system (2) when $\alpha = 2.6$, $\beta = 3$, $\gamma = 5$, $\delta = 1$, $k = 0.48$, $a = 1$, $3b = 0.4$, and $d = 0.2$: (a) projection on x–y plane, (b) projection on y–z plane, (c) projection on x–φ plane and (d) 3D view in the x–y–z plane.

map, and phase portraits. The system (2) can generate four-wing hyperchaotic attractors when $\alpha = 2.6$, $\beta = 3$, $\gamma = 5$, $\delta = 1$, $k = 0.48$, $a = 1$, $3b = 0.4$.

3.1. *The Lyapunov exponents*

The LEs which describe the rate of exponential divergence from perturbed initial conditions are a useful tool to quantify chaos. And two positive LEs are usually interpreted as an indication that the system is hyperchaotic. In this paper, we take the Dormand–Prince method (RK45) as the ODEs solver and use the famous Wolf method. The absolute and relative errors are kept to 10^{-6}, and the initial condition is set to (1, 1, 0, 0). The LEs are 1.245277, 0.682640, −0.078562 and −5.166089 when $d = 0.2$, and the numerical results are depicted in Fig. 1. And the phase portraits are shown in Fig. 2.

3.2. *The phase portraits and Poincaré section*

Another technique to distinguish a chaotic response from a regular one, the Poincaré mapping technique, as is well known, is proved to be very informative. A Poincaré section is often used to reduce a higher continuous system to a discrete map of lower dimension. For drawing the Poincaré map, we use an appropriate Poincaré section Ω defined by

$$\begin{aligned} \sum\nolimits_1 &= \{[x, y, z, \varphi]^T \in R4 \,|\, x = 0\} \\ \sum\nolimits_2 &= \{[x, y, z, \varphi]^T \in R4 \,|\, y = 0\} \\ \sum\nolimits_3 &= \{[x, y, z, \varphi]^T \in R4 \,|\, z = 0\} \\ \sum\nolimits_4 &= \{[x, y, z, \varphi]^T \in R4 \,|\, \varphi = 0\}. \end{aligned} \tag{9}$$

The Poincaré sections of the new system are provided in Fig. 3 for better analysis of the hyperchaotic system.

4. The Memristive Variable-Wing Attractors and Their Complex Dynamics

In this section, the phenomenon of variable-wing attractors will be studied. System (2) can also generate double-wing and three-wing chaotic attractors with different parameters except for four-wing attractors.

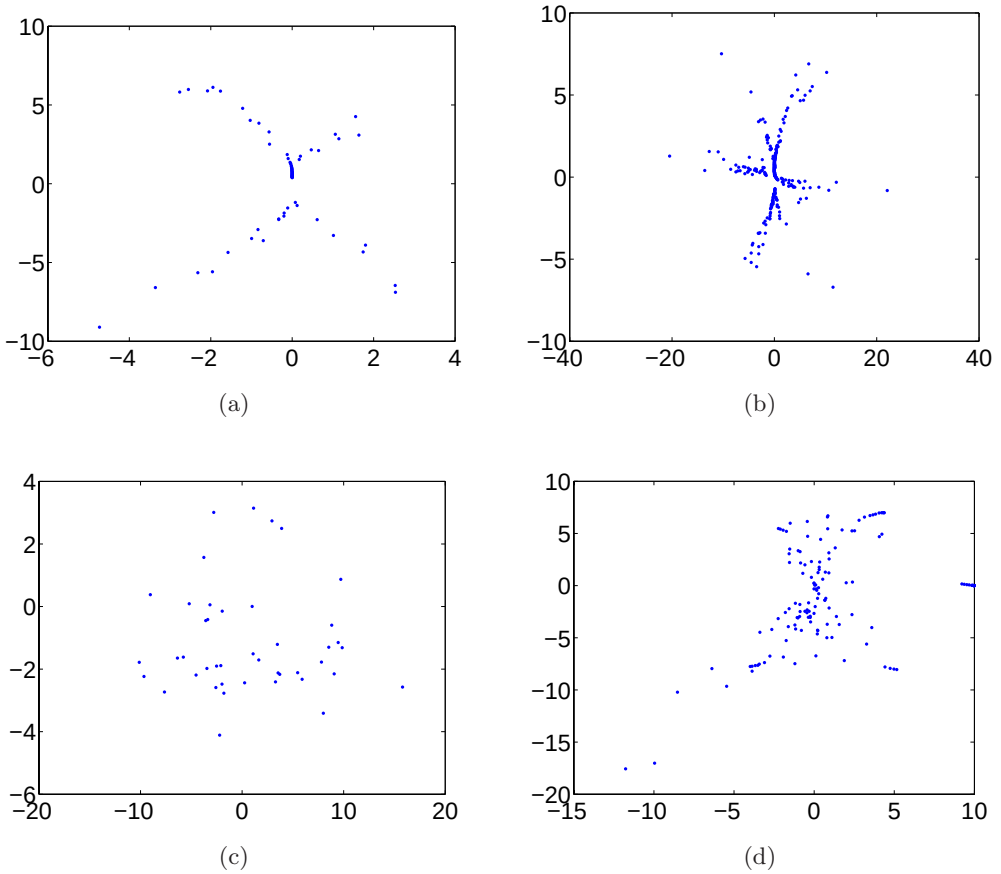

Fig. 3. Poincaré sections of system (2) when $\alpha = 2.6$, $\beta = 3$, $\gamma = 5$, $\delta = 1$, $k = 0.48$, $a = 1$, $3b = 0.4$, and $d = 0.2$: (a) projection on y–z plane when Poincaré section is $x = 0$, (b) projection on x–z plane when Poincaré section is $y = 0$, (c) projection on x–φ plane when Poincaré section is $z = 0$ and (d) projection on y–z plane when Poincaré section is $\varphi = 0$.

4.1. *Four-wing chaotic attractor*

When the parameters of system (2) are taken as $\alpha = 4$, $\beta = 6$, $\gamma = 10$, $\delta = 5$, $k = 0.48$, $a = 1$, $3b = 0.03$, the numerical results of LEs are depicted in Fig. 4 (the last one is not displayed because it is always a big negative number).

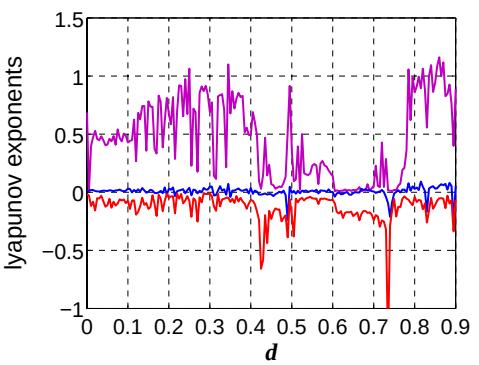

Fig. 4. First three LEs spectrum of system (2) versus d.

Table 1. Align the dynamic of system (2) with respect to d when the other parameters of system (2) are as follows: $\alpha = 4$, $\beta = 6$, $\gamma = 10$, $\delta = 5$, $k = 0.48$, $a = 1$, $3b = 0.03$.

d	(L_1, L_2, L_3, L_4)	Dynamic
$(0, 0.28]$	$(+, 0, -, -)$	Chaotic
$(0.28, 0.305)$	$(+, +, 0, -)$	Hyperchaotic
$(0.305, 0.605)$	$(+, 0, -, -)$	Chaotic
$(0.605, 0.7)$	$(0, 0, -, -)$	Torus
$[0.7, 0.74)$	$(+, 0, -, -)$	Chaotic
$[0.74, 0.75]$	$(0, -, -, -)$	Periodic orbits
$(0.75, 0.9)$	$(+, 0, -, -)$	Chaotic

From Fig. 4, we observe that the system (2) has complex dynamic behaviors such as chaos, hyperchaos, torus, and periodic orbits. Most of the dynamical systems can be characterized with their Lyapunov exponents (LEs), which are classified in Table 1.

Several simulations have been carried out based on the previous calculation on the changes of

Lyapunov exponents that go with the parameter d, the outcome of chaotic attractors with some typical parameters is summarized as follows:

(1) When $d = 0.2$, the phase portraits of system (2) shown in Fig. 5 are chaotic (the LEs are 0.449239, −0.000, −0.151118 and −11.287248).
(2) When $d = 0.3$, the phase portraits of system (2) shown in Fig. 6 are hyperchaotic (the LEs are 0.729418, 0.075176, 0.000 and −11.796949).
(3) When $d = 0.63$, the phase portraits of system (2) shown in Fig. 7 are torus (the LEs are 0.00, −0.00, −0.139672 and −10.853954).
(4) When $d = 0.74$, the phase portraits of system (2) shown in Fig. 8 are periodic orbits (the LEs are 0.00, −0.204139, −0.293670 and −10.502966).

4.2. *Three-wing chaotic attractors*

This new system can generate three-wing chaotic attractors by only varying a single parameter. Here parameter d is selected to be varied. If we choose the parameters $\alpha = 4$, $\beta = 6$, $\gamma = 10$, $\delta = 5$, $k = 0.48$, $a = 1$, $3b = 0.03$, and $d = 0.9$, three-wing chaotic attractors can be observed, as shown in Fig. 9.

4.3. *Coexisting two-wing chaotic attractors*

Multiple attractors mean that several attractors are created simultaneously from different initial values. This new system can generate coexisting two-wing chaotic attractors. If we choose the parameters $\alpha = 4$, $\beta = 6$, $\gamma = 10$, $\delta = 5$, $k = 0.48$, $a = 1$, $3b = 0.03$, and $d = 0.01$, system (2) can generate two neighboring two-wing chaotic attractors with initial values (±1, 10, 0, 0) as shown in Fig. 10.

4.4. *Time sequence of the variable-wing attractors*

In order to investigate the variable-wing attractors, we have a simulation for time series depicted in Fig. 11 when the parameters are taken as $\alpha = 4$, $\beta = 6$, $\gamma = 10$, $\delta = 5$, $k = 0.48$, $a = 1$, $3b = 0.03$. From the time series of state variables x, y, z, and φ, we found that the time-domain waveforms of two-wing, three-wing, and four-wing attractors are obviously different. Liu claimed that the system revealed a true four-wing attractor if some trajectory of the upper-attractor must travel through the plane $z = 0$, moving to the lower attractor; or other

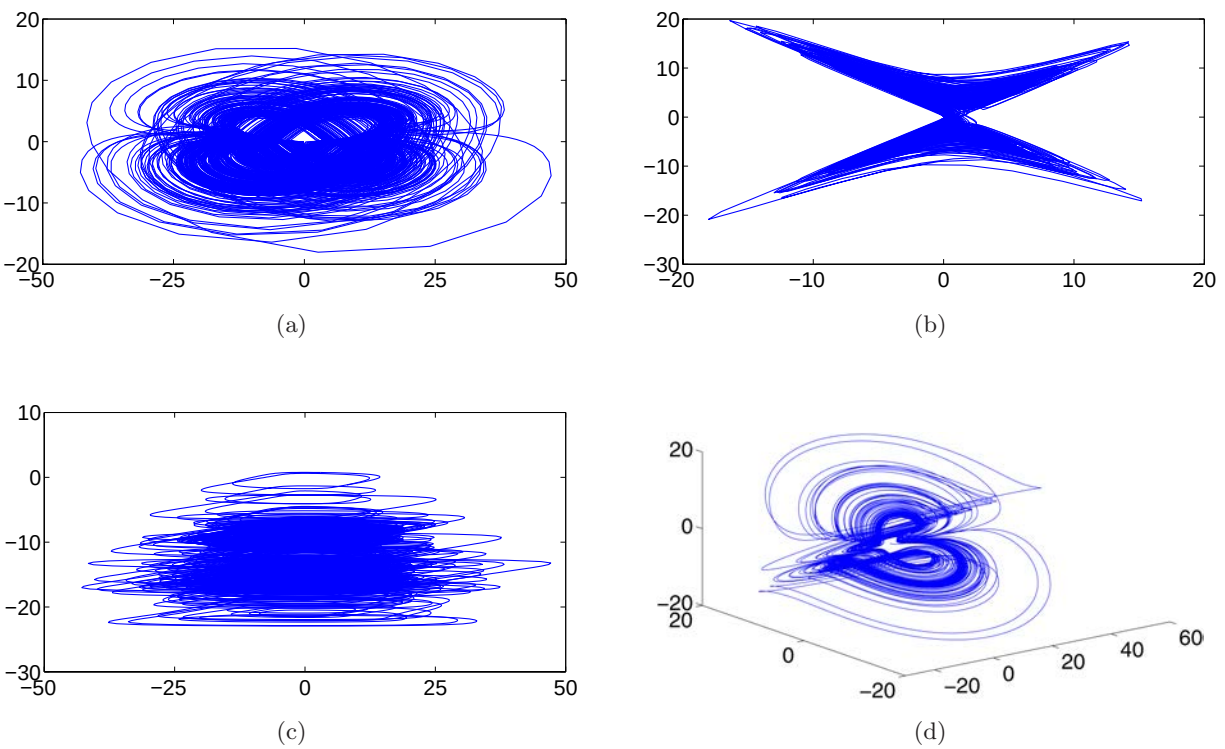

Fig. 5. Phase portraits of system (2) with $d = 0.2$: (a) projection on x–y plane, (b) projection on y–z plane, (c) projection on x–φ plane and (d) 3D view in the x–y–z plane.

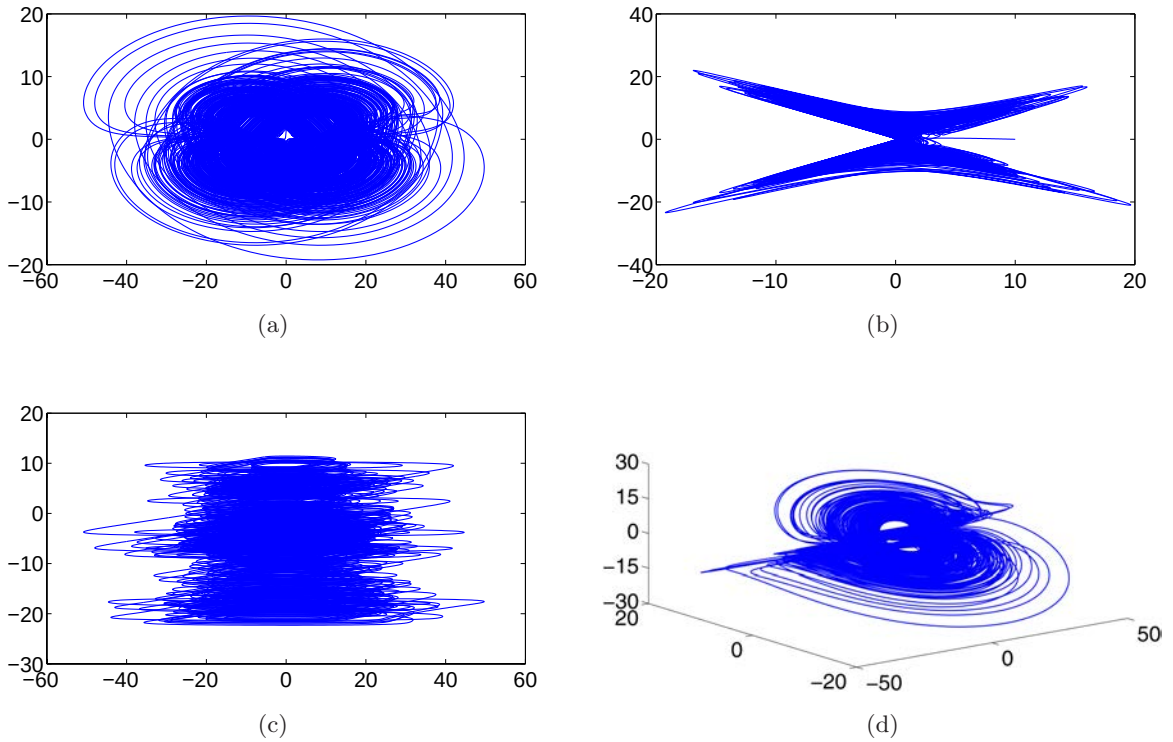

Fig. 6. Phase portraits of system (2) with $d = 0.3$: (a) projection on x–y plane, (b) projection on y–z plane, (c) projection on x–φ plane and (d) 3D view in the x–y–z plane.

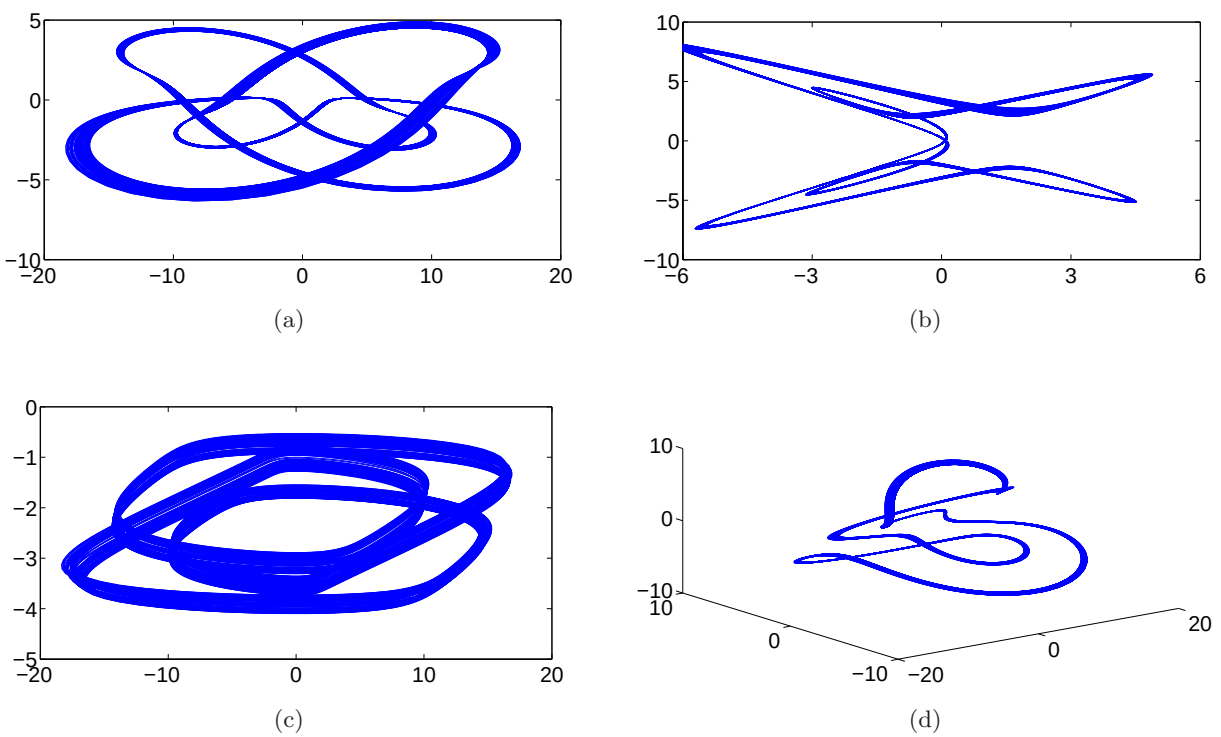

Fig. 7. Phase portraits of system (2) with $d = 0.63$: (a) projection on x–y plane, (b) projection on y–z plane, (c) projection on x–φ plane and (d) 3D view in the x–y–z plane.

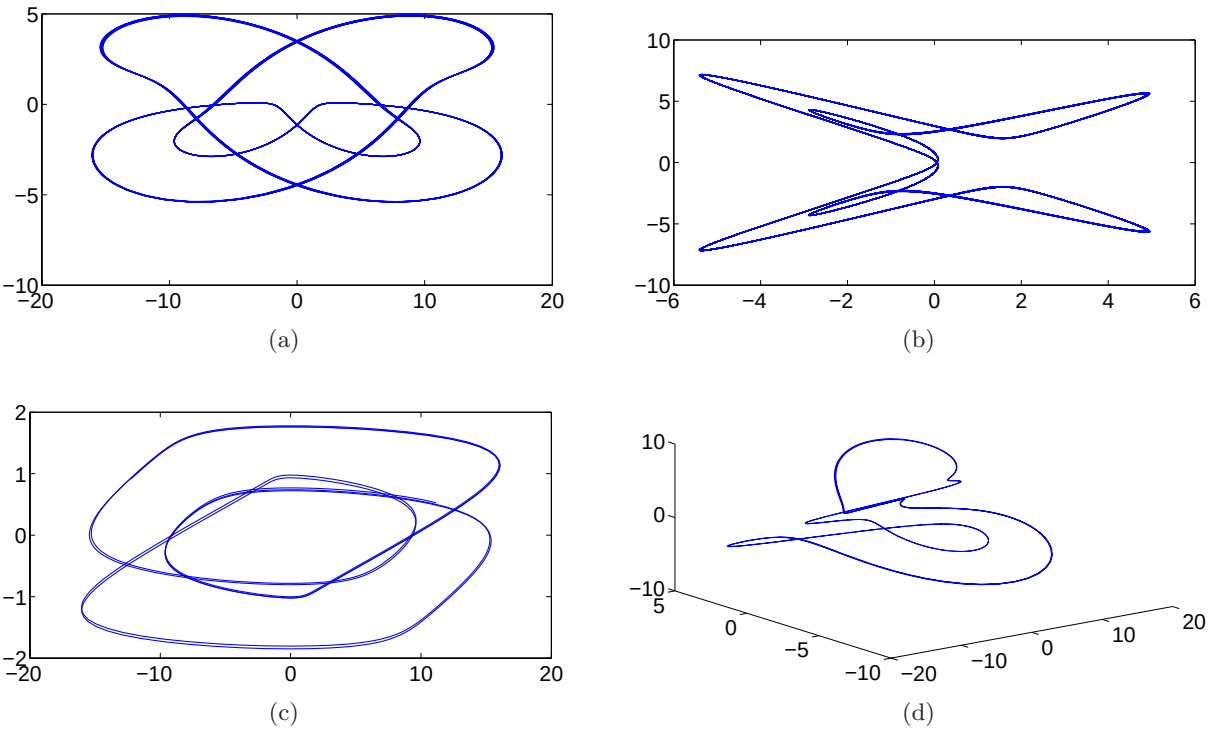

Fig. 8. Phase portraits of system (2) with $d = 0.74$: (a) projection on x–y plane, (b) projection on y–z plane, (c) projection on x–φ plane and (d) 3D view in the x–y–z plane.

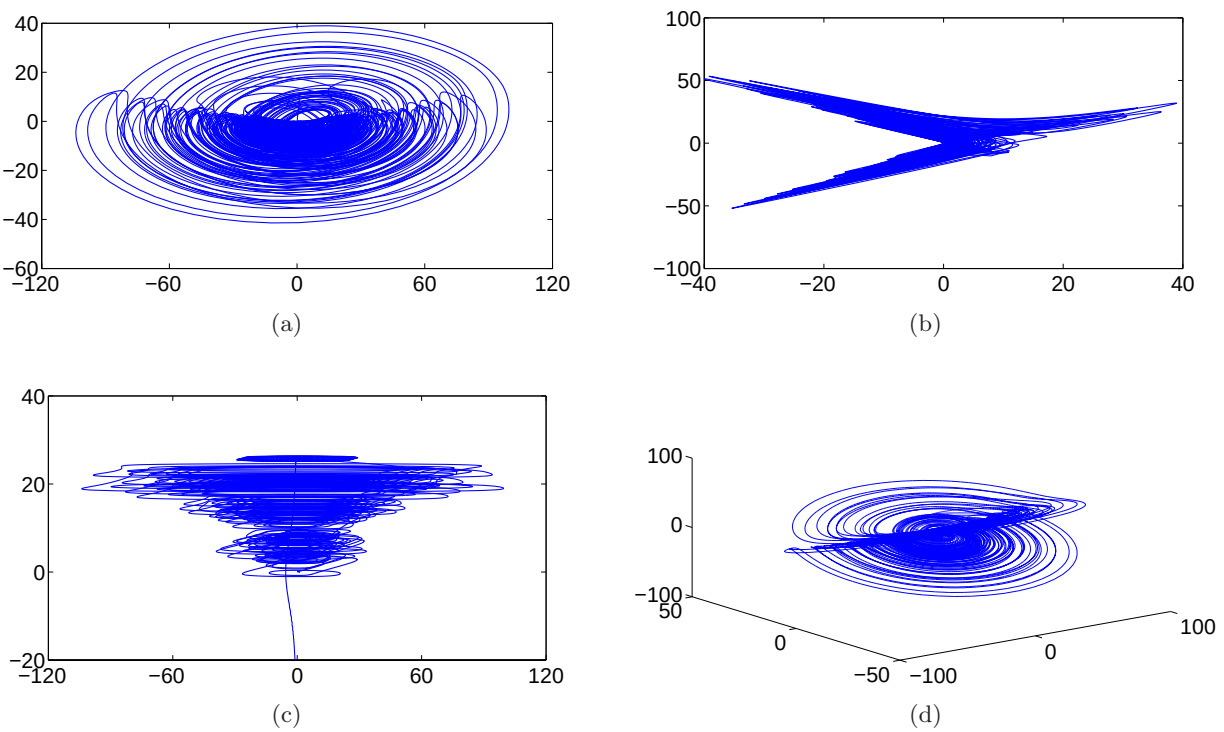

Fig. 9. Phase portraits of system (2) with $d = 0.9$: (a) projection on x–y plane, (b) projection on y–z plane, (c) projection on x–φ plane and (d) 3D view in the x–y–z plane.

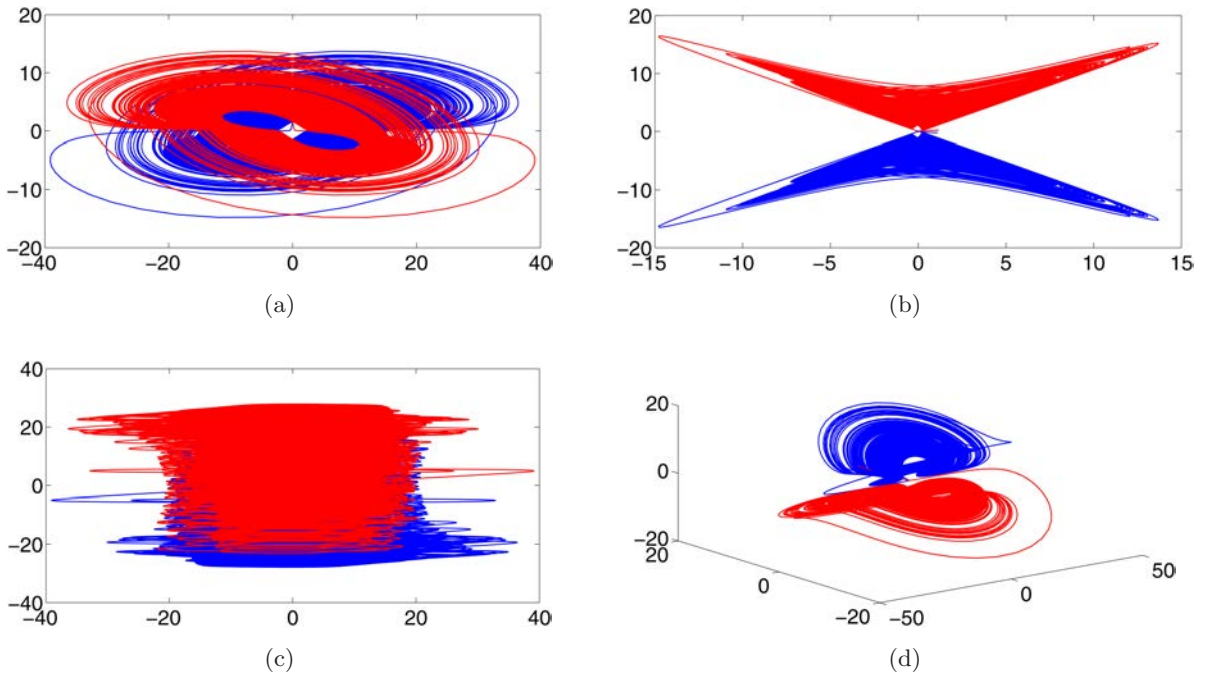

Fig. 10. Phase portraits of system (2) with $d = 0.01$: (a) projection on x–y plane, (b) projection on y–z plane, (c) projection on x–φ plane and (d) 3D view in the x–y–z plane.

way around [Liu & Chen, 2004]. From Fig. 11(c), we observe that the sign of variable z (colored in red) will change. According to the analyses above, the proposed system (2) is a true four-wing system.

4.5. *Coexisting multiple attractors, state transition, transient periodic orbits, and transient chaos*

When different initial states are considered, an interesting and striking phenomenon of multiple attractor behavior can be observed by numerical simulations. For different initial states, the projections of multiple attractors on the y–z plane are plotted in Fig. 12 when we choose the parameters $\alpha = 4$, $\beta = 6$, $\gamma = 10$, $\delta = 5$, $k = 0.48$, $a = 1$, $3b = 0.03$ and $d = 0.9$. When the initial states are [0.0001 10 1 10], the system (2) exhibits three-wing attractors, as shown in Fig. 12(a), while when the initial states are [0.001 10 0.01 1], the system (2) exhibits four-wing attractors, as shown in Fig. 12(b), while when the initial states are taken as [100 1.01 1 10.05], the system (2) exhibits

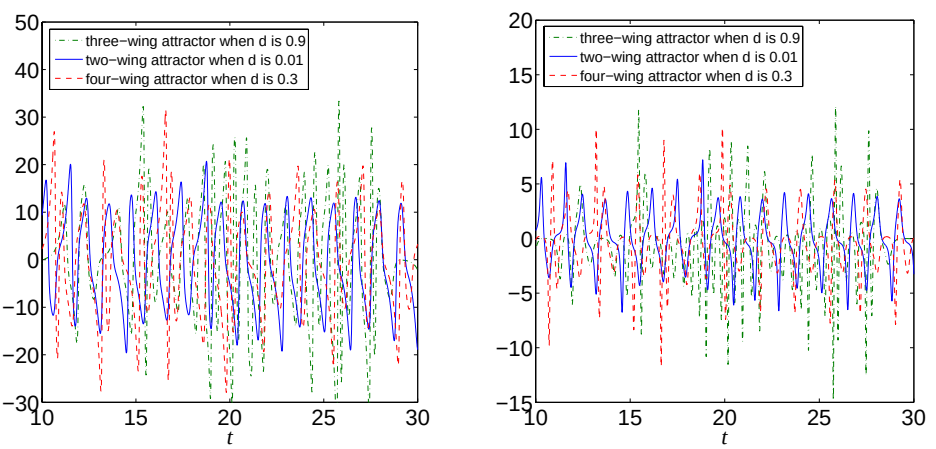

Fig. 11. Time sequence of the variable-wing attractor: (a) x, (b) y, (c) z and (d) φ.

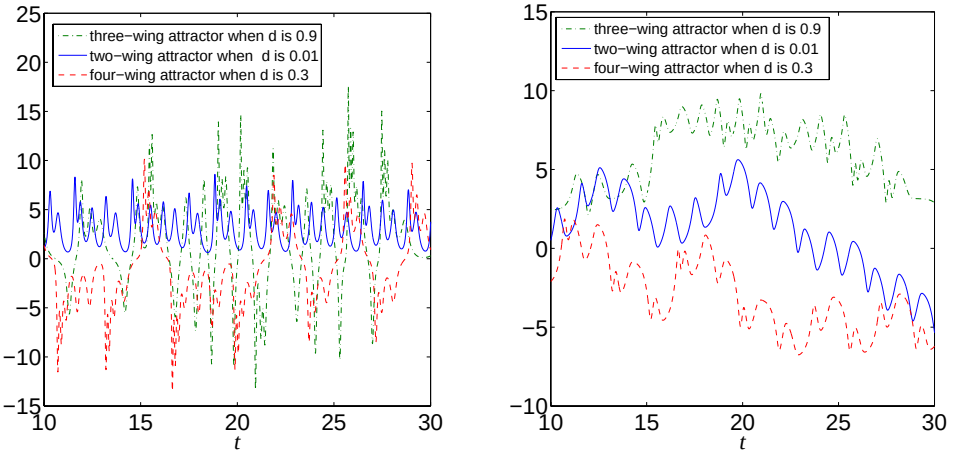

(c) (d)

Fig. 11. (*Continued*)

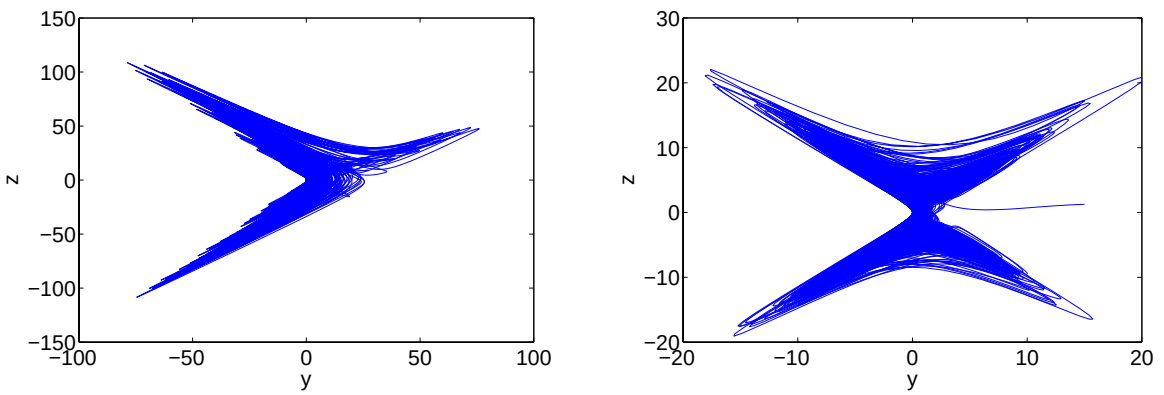

(a) (b)

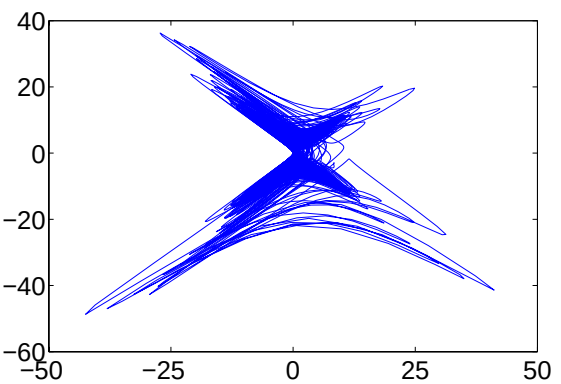

(c)

Fig. 12. The projections of multiple attractors on the y–z plane of system (2) with different initial states: (a) the initial states are taken as [0.0001 10 1 10], (b) the initial states are taken as [0.001 10 0.01 1] and (c) the initial states are taken as [100 1.01 1 10.05].

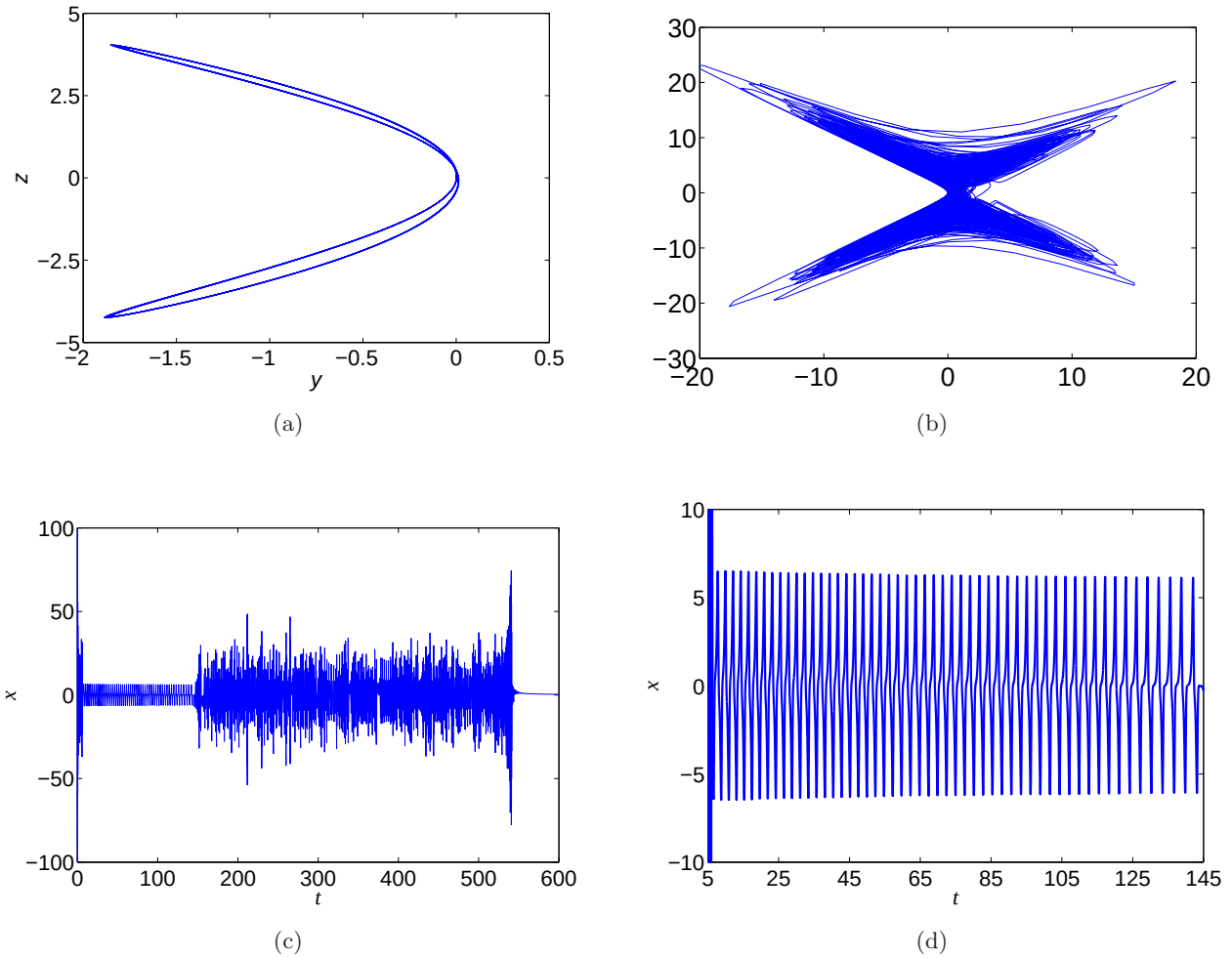

(a) (b) (c) (d)

Fig. 13. Transient chaos phenomenon of system (2): (a) phase portraits of system in time interval $(5, 145)$, (b) phase portraits of system in time interval $(145, 542)$, (c) orbit evolution with time $(0, 600)$ and (d) time series of system in time interval $(5, 145)$.

the attractors with state transition [Mou *et al.*, 2016] in Fig. 12(c). Sometimes there is no stable state in this system, but it has different dynamical behaviors when it starts from different dynamic time. From Fig. 13, we can find the state transition distinctly. At first, the orbits of the system are in transient periodic orbits as shown in Fig. 13(a), and then it transforms into transient chaotic orbits abruptly at about $t = 145$ sec shown in Fig. 13(b), and finally, it disappears at about $t = 542$ sec. With the time evolution, the system (2) has very complicated dynamical characteristics. The three different types of attractors coexist peacefully in this memristive system, which shows that the memristive system has high sensitivity to initial values and exhibits complex dynamical behaviors with multistability in the selected parameter region.

5. Circuit Implementation

In order to further observe the hyperchaotic four-wing attractor, the circuit implementation using operational amplifiers and multipliers is carried out. All operational amplifiers are selected as TL082. Their supply voltages are $E = \pm 15\,\mathrm{V}$. All the multipliers are of type AD633JN, which have laser-trimmed accuracy between $-10\,\mathrm{V}$ to $10\,\mathrm{V}$. However, the values of x, y, and z in Fig. 2 may exceed this range. By taking a time scale factor RC on the dimensionless time, the system (2) after scale transformation can be described as follows:

$$\begin{cases} RC\dot{x} = \alpha x - 10\beta yz \\ RC\dot{y} = -\gamma y + 10xz \\ RC\dot{z} = 10xy - \delta z - d(a + 100 \times 3b\varphi^2)x \\ RC\dot{\varphi} = kx. \end{cases} \tag{10}$$

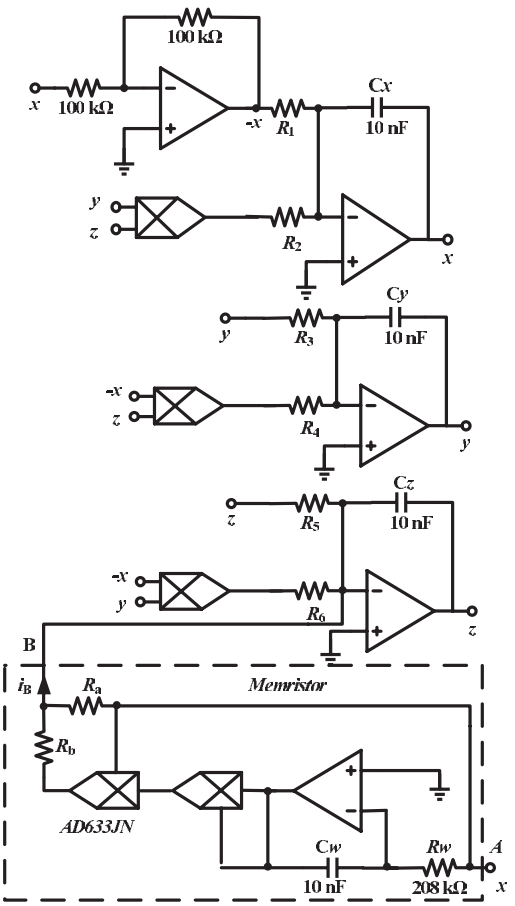

Fig. 14. Circuit diagram of memristive four-wing system.

We adopt a simple flux-controlled memristor [Li *et al.*, 2015] depicted in the dashed boxes of Fig. 14 with classical components, and verify the hyperchaotic dynamics at $d = 0.2$. The electronic circuit is shown in Fig. 14. By putting a multiplication factor 0.1/V on each multiplication with AD633JN, the state equations can be obtained as follows:

$$\begin{cases} C_x\dot{v}_x = \dfrac{v_x}{R_1} - \dfrac{v_y v_z \cdot 0.1/\mathrm{V}}{R_2} \\ C_y\dot{v}_y = \dfrac{-v_y}{R_3} + \dfrac{v_x v_z \cdot 0.1/\mathrm{V}}{R_4} \\ C_z\dot{v}_z = \dfrac{v_x v_y \cdot 0.1/\mathrm{V}}{R_6} - \dfrac{v_z}{R_5} \\ \qquad\quad - \left(\dfrac{v_x}{R_a} + \dfrac{v_x {v_\varphi}^2}{R_b} 0.1/\mathrm{V} \cdot 0.1/\mathrm{V}\right) \\ C_\varphi\dot{v}_\varphi = \dfrac{v_x}{R_w} \end{cases} \tag{11}$$

where v_x, v_y, v_z and v_φ are the voltages on capacitors. Compared with (10) and (11), the parameters are taken as follows: $C_x = C_y = C_z = C$, $R_1 = R/\alpha$, $R_2 = 0.01R/\beta$, $R_3 = R/\gamma$, $R_4 = 0.01R$, $R_5 = R/\delta$, $R_6 = 0.01R$. Now, let us take $R = 100\,\mathrm{k}\Omega$ and $C = 10\,\mathrm{nF}$. According to the parameters of the system, i.e. $\alpha = 2.6$, $\beta = 3$, $\gamma = 5$, and $\delta = 1$, so $R_1 = 38.46\,\mathrm{k}\Omega$, $R_2 = 333.3\,\Omega$, $R_3 = 20\,\mathrm{k}\Omega$, $R_4 = 1\,\mathrm{k}\Omega$, $R_5 = 100\,\mathrm{k}\Omega$, $R_6 = 1\,\mathrm{k}\Omega$.

In the memristor model, if we take $Cw = C$ and $k = 0.48$, then it is not hard to see that

$$R_w = \frac{R}{k}, \quad R_a = \frac{R}{da}, \quad R_b = \frac{R}{10\,000d(3b)}. \tag{12}$$

When $a = 1$, $3b = 0.4$ and $d = 0.2$, it can be obtained: $R_w = 208\,\mathrm{k}\Omega$, $R_a = 192.3\,\mathrm{k}\Omega$, and $R_b = 125\,\Omega$. Figure 15 shows the oscilloscope traces from

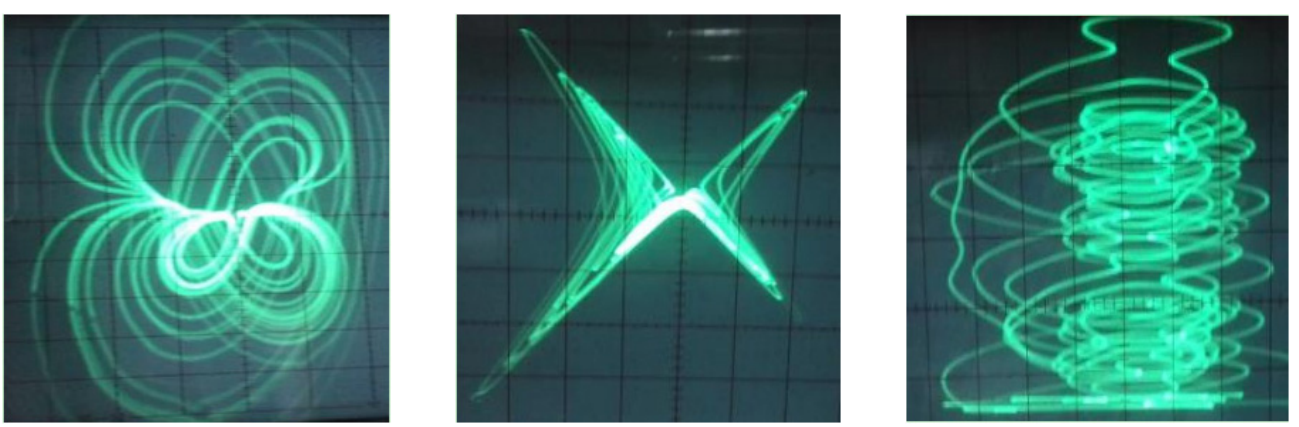

(a) (b) (c)

Fig. 15. Phase portraits of system (2) observed from oscilloscope: (a) projection on x–y plane, (b) projection on y–z plane and (c) projection on x–φ plane.

this memristive circuit. The results are in agreement with Fig. 2.

6. Conclusion

Through only adding a flux-controlled memristor, a hyperchaotic four-wing system with smooth nonlinearity is proposed in this paper. The most striking feature is that the newly proposed system can not only generate hyperchaotic four-wing attractors but also generate two-to-four-wing chaotic attractors by only changing the parameter d. Moreover, the coexisting multiple attractors (e.g. three-wing attractors, four-wing attractors and the attractors with state transition under the same system parameters) are numerically simulated. The complex dynamics behaviors are verified by theoretical analysis and numerical simulation. And we carry out the circuit implementation of the new memristive system.

Acknowledgments

This work is supported by the National Natural Science Foundation of China (No. 61274020), the Natural Science Foundation of Hunan Province, China (No. 2016JJ2030), the Open Fund Project of Key Laboratory in Hunan Universities No. 15K027 and the science and technology planned project of YongZhou City.

References

Adhikari, S. P., Kim, H., Budhathoki, R. K., Yang, C. J. & Chua, L. O. [2015] "A circuit-based learning architecture for multilayer neural networks with memristor bridge synapses," *IEEE Trans. Circuits Syst.-I: Regul. Pap.* **62**, 215–223.

Bao, B. C., Xu, J. P., Zhou, G. H., Ma, Z. H. & Zou, L. [2011] "Chaotic memristive circuit: Equivalent circuit realization and dynamical analysis," *Chin. Phys. B* **20**, 120502.

Bao, B. C., Hu, F. W., Liu, Z. & Xu, J. P. [2014] "Mapping equivalent approach to analysis and realization of memristor-based dynamical circuit," *Chin. Phys. B* **23**, 303–310.

Bao, B. C., Jiang, P., Wu, H. G. & Hu, F. W. [2015] "Complex transient dynamics in periodically forced memristive Chua's circuit," *Nonlin. Dyn.* **79**, 2333–2343.

Cang, S. J., Wu, A. G., Wang, Z. H., Xue, W. & Chen, Z. Q. [2016] "Birth of one-to-four-wing chaotic attractors in a class of simplest three-dimensional continuous memristive systems," *Nonlin. Dyn.* **83**, 1987–2001.

Chua, L. O. [1971] "Memristor-the missing circuit element," *IEEE Trans. Circuit Th.* **18**, 507–519.

Dadras, S. & Momeni, H. R. [2009] "A novel three-dimensional autonomous chaotic system generating two-, three- and four-scroll attractors," *Phys. Lett. A* **373**, 3637–3642.

Dadras, S., Reza Momeni, H., Qi, G. Y. & Wang, Z. L. [2012] "Four-wing hyperchaotic attractor generated from a new 4D system with one equilibrium and its fractional-order form," *Nonlin. Dyn.* **67**, 1161–1173.

Duan, S., Hu, X., Dong, Z., Wang, L. & Mazumder, P. [2015] "Memristor-based cellular nonlinear/neural network: Design, analysis, and applications, neural networks and learning systems," *IEEE Trans. Neural Netw. Learn. Syst.* **26**, 1202–1213.

Iu, H. H. C., Yu, D. S., Fitch, A. L., Sreeram, V. & Chen, H. [2011] "Controlling chaos in a memristor based circuit using a twin-T notch filter," *IEEE Trans. Circuits Syst.-I: Regul. Pap.* **58**, 1337–1343.

Li, Q. D., Zeng, H. Z. & Li, J. [2015] "Hyperchaos in a 4D memristive circuit with infinitely many stable equilibria," *Nonlin. Dyn.* **79**, 2295–2308.

Lin, Z. S., Yu, S. M., Lü, J. H., Cai, S. T. & Chen, G. R. [2015] "Design and ARM-embedded implementation of a chaotic map-based real-time secure video communication system," *IEEE Trans. Circuits Syst. Vid. Technol.* **25**, 1203–1216.

Liu, W. & Chen, G. R. [2003] "A new chaotic system and its generation," *Int. J. Bifurcation and Chaos* **13**, 261–267.

Liu, W. & Chen, G. R. [2004] "Can a three-dimensional smooth autonomous quadratic chaotic system generate a single four-scroll attractor?" *Int. J. Bifurcation and Chaos* **14**, 1395–1405.

Lü, J. H. & Chen, G. R. [2002] "A new chaotic attractor coined," *Int. J. Bifurcation and Chaos* **12**, 659–661.

Ma, J., Chen, Z. Q., Wang, Z. L. & Zhang, Q. [2015] "A four-wing hyper-chaotic attractor generated from a 4D memristive system with a line equilibrium," *Nonlin. Dyn.* **81**, 1275–1288.

Mou, J., Sun, K. H., Ruan, J. Y. & He, S. B. [2016] "A nonlinear circuit with two memcapacitors," *Nonlin. Dyn.* **86**, 1735–1744.

Muthuswamy, B. [2010] "Implementing memristor based chaotic circuits," *Int. J. Bifurcation and Chaos* **20**, 1335–1350.

Qi, G. Y., Chen, G. R., van Wyk, M. A., van Wyk, B. J. & Zhang, Y. H. [2008] "A four-wing chaotic attractor generated from a new 3D quadratic autonomous system," *Chaos Solit. Fract.* **38**, 705–721.

Rakkiyappan, R., Sivasamy, R. & Li, X. D. [2015] "Synchronization of identical and nonidentical memristor-based chaotic systems via active backstepping control technique," *Circuits Syst. Sign. Process.* **34**, 763–778.

Samuel, G. [2016] "Better memory," *Commun. ACM* **59**, 23–25.

Strukov, D. B., Snider, G. S., Stewart, D. R. & Williams, R. S. [2008] "The missing memristor found," *Nonlin. Dyn.* **453**, 80–83.

Teng, L., Iu, H. H. C., Wang, X. Y. & Wang, X. K. [2014] "Chaotic behavior in fractional-order memristor-based simplest chaotic circuit using fourth degree polynomial," *Nonlin. Dyn.* **77**, 231–241.

Wang, L. [2009] "3-scroll and 4-scroll chaotic attractors generated from a new 3D quadratic autonomous system," *Nonlin. Dyn.* **56**, 453–462.

Wang, Q. X., Yu, S. M., Li, C. Q., Lü, J. H., Fang, X. L., Guyeux, C. & Bahi, J. M. [2016] "Theoretical design and FPGA-based implementation of higher-dimensional digital chaotic systems," *IEEE Trans. Circuits Syst.-I* **63**, 401–412.

Wu, R. P. & Wang, C. H. [2016] "A new simple chaotic circuit based on memristor," *Int. J. Bifurcation and Chaos* **26**, 1650145-1–11.

Yu, S. M., Tang, W. K. S., Lü, J. H. & Chen, G. R. [2010] "Generating $2n$-wing attractors from Lorenz-like systems," *Int. J. Circ. Theor. Appl.* **38**, 243–258.

Yu, F., Wang, C. H., Yin, J. W. & Xu, H. [2011a] "Novel four-dimensional autonomous chaotic system generating one-, two-, three- and four-wing attractors," *Chin. Phys. B* **20**, 110505-1–7.

Yu, S. M., Lü, J. H., Chen, G. R. & Yu, X. H. [2011b] "Generating grid multiwing chaotic attractors by constructing heteroclinic loops into switching systems," *IEEE Trans. Circuits Syst.-II*: *Exp. Briefs* **58**, 314–318.

Yuan, F., Wang, G. Y. & Wang, X. W. [2016] "Extreme multistability in a memristor-based multi-scroll hyper-chaotic system," *Chaos* **26**, 1–13.

Zarei, A. [2016] "Complex dynamics in a 5D hyper-chaotic attractor with four-wing, one equilibrium and multiple chaotic attractors," *Nonlin. Dyn.* **61**, 585–605.

Zhang, C. X. & Yu, S. M. [2013] "On constructing complex grid multiwing hyperchaotic system: Theoretical design and circuit implementation," *Int. J. Circ. Theor. Appl.* **41**, 221–237.

Zhou, L., Wang, C. H. & Zhou, L. L. [2016] "Generating hyperchaotic multi-wing attractor in a 4D memristive circuit," *Nonlin. Dyn.* **85**, 2653–2663.